GDCh Communications Angewandte Chemie International Edition www.angewandte.org

How to cite: *Angew. Chem. Int. Ed.* **2024**, *63*, e202318428
doi.org/10.1002/anie.202318428

Barium Complexes | Hot Paper

Metal Vapour Synthesis of an Organometallic Barium(0) Synthon

*Oliver P. E. Townrow, Christian Färber, Ulrich Zenneck, and Sjoerd Harder**

Dedicated to Professor Rhett Kempe on the occasion of his 60th birthday

Abstract: A hydrocarbon-soluble barium anthracene complex was prepared by means of metal vapour synthesis. Reaction of 9,10-bis(trimethylsilyl)anthracene (Anth″) with barium vapour gave deep purple Ba(Anth″) which after extraction with diethyl ether crystallised as the cyclic octamer $[Ba(Anth'')\cdot Et_2O]_8$. Dissolution in benzene or toluene led to replacement of the Et_2O ligand with a softer arene ligand and isolation of Ba(Anth″)·arene. Diffusion ordered spectroscopy (DOSY NMR) measurements in benzene-d_6 indicate solution species with a molecular weight that equals a trimeric constitution. Natural population analysis (NPA) assigned charges of +1.70 and −1.70 to Ba and Anth″, respectively, relating to highly ionic Ba^{2+}/$Anth''^{2-}$ bonding. Preliminary reactivity studies with air, $Ph_2C{=}NPh$, or H_2 show that the complex reacts as a Ba^0 synthon by release of neutral Anth″. This soluble molecular Ba^0/Ba^{II} redox synthon provides new routes for the syntheses of barium complexes under mild conditions.

The alkaline-earth metals (Ae) are among the most abundant elements on earth, have low electronegativity, and produce highly reactive ionic complexes typically in the +II oxidation state.[1] Apart from their applications in homogeneous catalysis,[2] a major focus has been on their lower oxidation states and subsequent uses in bond activation.[3] Although there has been quite some progress in the chemistry of Be and Mg in the +I or 0 oxidation states (Scheme 1, **I**–**V**),[5] there is only a single example of a Ca^{I} complex (**VI**).[6] Heavy Ae^0 complexes $Ae(N_2)_8$, $Ae(CO)_8$, and $Ae(C_6H_6)_3$ (Ae = Ca, Sr, Ba) have been isolated and detected, however only in a neon matrix at 12 K.[7] In these and aforementioned complexes (e.g. **I**, **II** or **VI**), a large proportion of the metal's valence electrons are delocalised over the ligands resulting in metal oxidation state ambiguities.[8–10]

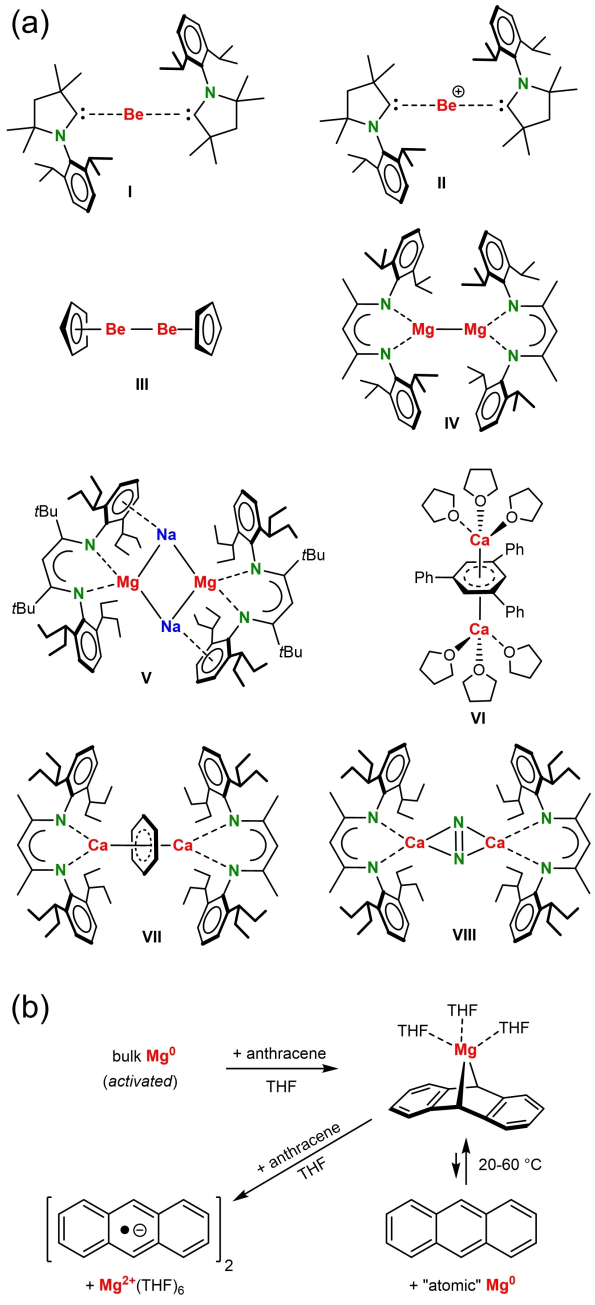

Scheme 1. Low-valent Ae metal complexes and synthons. (a) Formulas **I**–**VIII**. (b) Synthesis and reactivity of Mg(anthracene) according to Ramsden and Bogdanović.

[*] Dr. O. P. E. Townrow, Dr. C. Färber, Prof. Dr. U. Zenneck, Prof. Dr. S. Harder
Inorganic and Organometallic Chemistry, Universität Erlangen-Nürnberg
Egerlandstrasse 1, 91058 Erlangen (Germany)
E-mail: sjoerd.harder@fau.de

Preparing well-defined complexes of the heavier Ae metals in low oxidation states has been found to be extremely challenging due to drastic reactivity increases from Be to Ba. In addition, the increase in metal size makes it progressively more difficult to implement superbulky ligands to achieve complex stabilisation. For example, the attempted synthesis of the heavier Ca^I analogue of **IV** led either to reduction of the aromatic solvent (**VII**) or rapid N_2 activation (**VIII**), even at temperatures as low as $-50\,°C$.[11] In the context of small molecule activation, the participation of *d*-orbitals for Ca, Sr, and especially for Ba has been controversially discussed,[10–12] however, was also found to be not crucial.[13,14] Although **VII** and **VIII** should be formulated as species in which $C_6H_6^{2-}$ or N_2^{2-} anions bridge two Ca^{2+} ions, with few exceptions, these binuclear complexes generally react as Ca^I synthons by elimination of benzene or N_2 delivering one electron per Ca centre for substrate reduction.[11,15,16]

Development of Ae^0 synthons, i.e. formal Ae^{2+} species that react reductively like the bare Ae^0 metal, would enable two-electron reduction at a single metal centre. One such complex, Mg(Anth) (Anth = anthracene), was first described in 1965 by Ramsden,[17] and its chemistry was further developed by Bogdanović.[18] This compound crystallises from THF as the monomer $Mg(Anth)\cdot(THF)_3$ (**IX**) in which Mg^{2+} bridges the 9 and 10 carbon positions of a bent anthracene dianion (Scheme 1b).[19] The complex is in equilibrium with neutral anthracene and a form of highly reactive "atomic" Mg^0. The presence of excess anthracene can also result in the formation of an anthracene radical anion.[20] As a source of soluble zerovalent magnesium, **IX** has enabled the facile syntheses of challenging Grignard reagents,[21] transition metal salt reductions,[22] and is an excellent medium for hydrogen storage in the presence of a transition metal catalyst ($Mg^0 + H_2 \leftrightarrow MgH_2$).[23]

Extension of this work to the heavier Ae metals would not only enrich low-valent *s*-block metal chemistry but also provide new key reagents in Ae metal chemistry. Although syntheses of Ae(Anth) (Ae = Ca, Sr, Ba) have been previously described, experimental details such as colour and composition are contradicting.[24–26] As these complexes are sparingly soluble, their analysis has been restricted to FT-IR, UV/Vis, and solid-state ^{13}C NMR spectroscopy as well as inconclusive quench experiments.[26] Herein, we report on the synthesis, structure and full characterisation of a Ba anthracene complex and its preliminary reactivity as a Ba^0 synthon.

To improve solubility and stability, we aimed for the reduction of 9,10-bis(trimethylsilyl)anthracene (Anth″) with Ba^0 (Scheme 2). As pointed out earlier by Lehmkuhl *et al.*,[27] the −M effect of a Me_3Si-substituent (negative hyperconjugation) is larger than the +I inductive effect and consequently Anth″ is easier to reduce than Anth, enhancing complex stability. Indeed, Raston and co-workers reported the monomeric structure of $Mg(Anth'')\cdot(THF)_2$ and showed that its decomposition into Mg^0 and Anth″ is much slower than that of **IX**.[28] Despite the more facile reduction of Anth″, and the more negative reduction potential of Ba^0 ($E^0 = -2.92$ V *vs.* NHE) *vs.* Mg^0 ($E^0 = -2.36$ V *vs.* NHE),[29] the reaction between Ba^0 and Anth″ in benzene was found to be extremely slow (Figure S1). Even with mechanochemical activation or the use of highly activated Ba^0 obtained by co-condensation with heptane using a method reported by Timms,[30] no satisfactory conversions were obtained. It is well-known that the poor reactivity of the heavier Ae^0 elements, in combination with the very high reactivity of its compounds,[31] obstructs complex syntheses directly from the metal.[32] This difference with the very facile synthesis of Mg compounds, e.g. Grignard reagents, can be explained by the unusually low atomisation enthalpy of Mg^0 (35.3 kcal mol^{-1}), relative to Ba^0 (43.0 kcal mol^{-1}).[33] This led us to probe the synthesis of Ba(Anth″) by metal vapour synthesis (MVS), a method which brings the ligand in contact with discrete metal atoms. The direct reaction with metal atoms instead of with bulk metal has the advantage of starting at a higher free energy level which is closer to the transition state by approximately the free energy of metal sublimation (Scheme 2a).[30b, 34] These thermodynamic and kinetic advantages enable access to compounds which cannot be prepared by any other

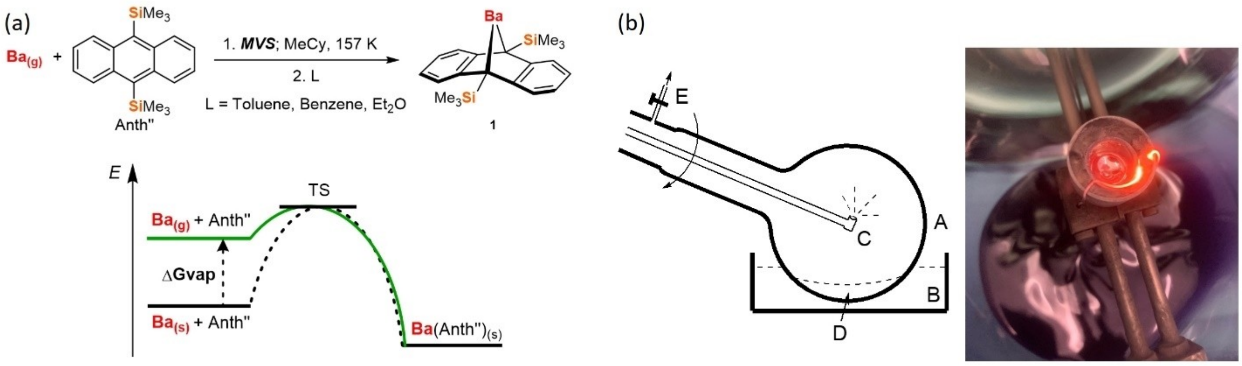

Scheme 2. (a) Reaction of Ba^0 vapour with Anth″ to give **1**. (b) Left: Diagram of the rotary metal evaporator reactor used in the synthesis of [Ba(Anth″)] (**1**). A = reaction vessel (2 L, ≈7×10^{-4} mbar), B = coolant (EtOH/liquid N_2, −116 °C), C = Ba metal in crucible heated by a resistive tungsten coil, D = Anth″ in MeCy, E = valve for Schlenk line connection after synthesis. Right: Photograph during the reaction, showing vaporising liquid Ba in the resistively heated crucible. Note the deep purple suspension of **1** in the background.

means,[35] and previously allowed the synthesis of Ba(COT)·(THF)$_n$ (COT = cyclooctatetraene).[36]

As Anth″ is poorly volatile, we converted a rotary evaporator into an MVS reactor to vaporise the metal atoms directly into a cooled solution of ligand (Scheme 2b).[37] The rotating reactor vessel provides a continuously replenishing film of ligand solution to the vaporised metal atoms under temperature-controlled conditions. Metallic Ba^0 was evaporated from a resistively heated crucible (7×10^{-4} mbar) into a methylcyclohexane solution of excess Anth″. Over the course of an hour, a fine deep purple suspension of Ba(Anth″) (**1**) was formed, and following filtration and extraction of the residue with either benzene, toluene, or diethyl ether; deep purple solutions of Ba(Anth″)·L (**1·L**; L = Arene, Et_2O) were obtained (Scheme 2b). In contrast to Mg(Anth″)·(THF)$_2$ (**IX**), which is stabilised by THF,[18] extraction of Ba(Anth″) with THF or THP (tetrahydropyran) led to formation of a dark, insoluble, hitherto undefined precipitate. Dependent on vaporisation rate and ligand concentration, typical isolated yields of **1·L** are around 32 % relative to Ba^0. The product is highly sensitive to air and moisture, and unstable to extensive drying *in vacuo*, the toluene adduct being the most stable to the latter. In contrast to the co-condensation of Ca^0 and benzene, where Ca^0 inserted in the benzene C–H bond to produce PhCaH,[38] no evidence for such a process is observed here.

Whilst crystallisations from benzene or toluene only produced microcrystalline needles of Ba(Anth″)·arene (**1·benzene** or **1·toluene**) unsuitable for X-ray diffraction, crystallisation from diethyl ether gave dark purple crystals of Ba(Anth″)·Et_2O (**1·Et$_2$O**) of good quality. The crystal structure shows a cyclic octamer in which Ba is sandwiched between two Anth″ ligands by η^4-coordination to a central ring and η^6-coordination to a flanking ring (Figure 1). Additional coordination of Et_2O creates a bent sandwich which induces the curvature needed for cyclisation. As all Ba atoms lie in the mirror plane and Ba–Ba'-Ba angles vary between 134.74(2)° and 135.26(2)° with Ba–Ba' distances of 6.3061(4) Å to 6.3327(4) Å, they span a nearly perfect octagon with ideal angles of 135°. This is in contrast to the recently reported cyclic structure of octameric [Ba(Cbz)SiH$_3$]$_8$ (Cbz is a bulky carbazolide ligand)[39] in which the ring is non-planar and irregular. Prerequisites for the self-assembly of such circular aggregates are a combination of large and small ligands, or formation of a polymeric bent supersandwich both leading to curvature and ring formation. Thus, dodenuclear Mg_{12} clusters have been isolated,[40] and most recently even larger cyclic M_{18} supersandwiches were crystallised (M = Sr, Sm, Eu).[41]

The planarity and bond lengths of the two different symmetry independent Anth″ anions in **1·Et$_2$O** (Figure 2) are more similar to the structures of neutral Anth″ or the Anth″$^{\bullet-}$ radical anion than Anth″$^{2-}$ in Mg(Anth″)·(THF)$_2$ (Figure S24).[27,28,42] This observation should not lead to conclusions on ligand charge, which is closer to −2 than −1 (see below), but is related to the large size and low electronegativity of Ba resulting in highly ionic multihapto Ba-Anth″ bonding. The more covalent Mg–C bonds in Mg(Anth″)·(THF)$_2$ result in rehybridisation of C towards sp^3.

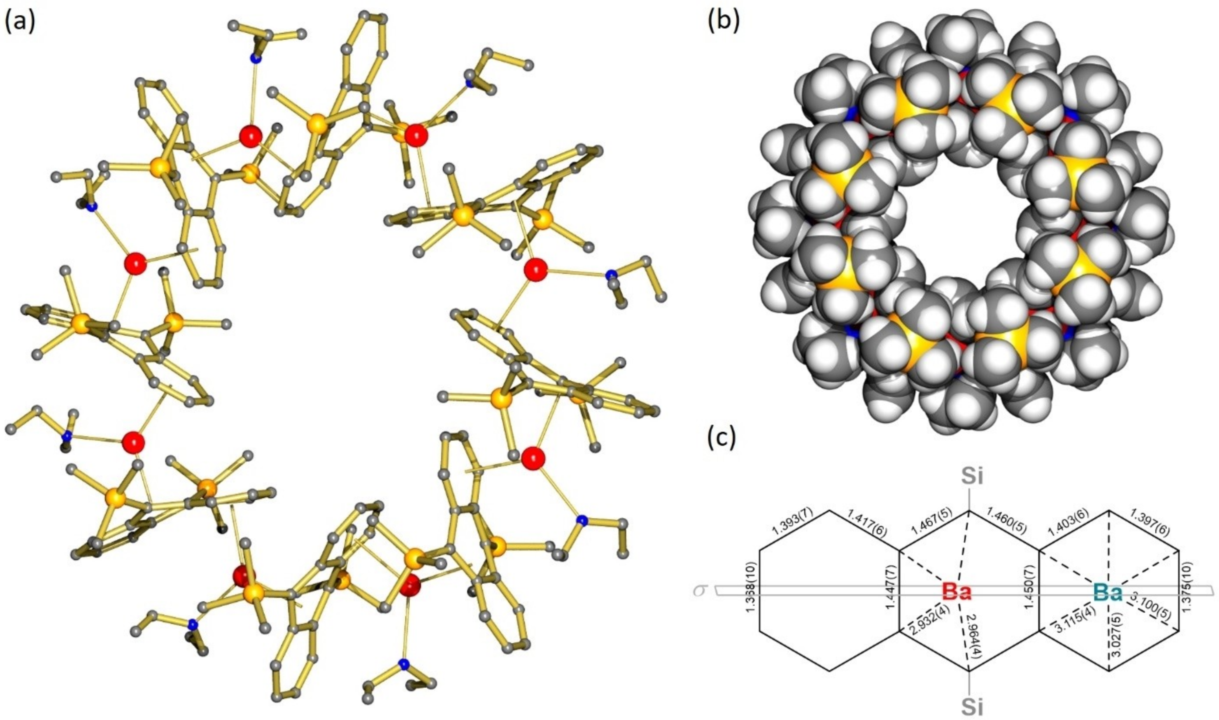

Figure 1. (a) Crystal structure of the octameric complex [Ba(Anth″)·Et_2O]$_8$ (**1·Et$_2$O**); H atoms excluded for clarity (Ba red, Si orange, O blue). (b) Space-filling model for **1·Et$_2$O**. (c) Selected Ba–C and C–C bond lengths (Å) for centrosymmetric **1·Et$_2$O**.

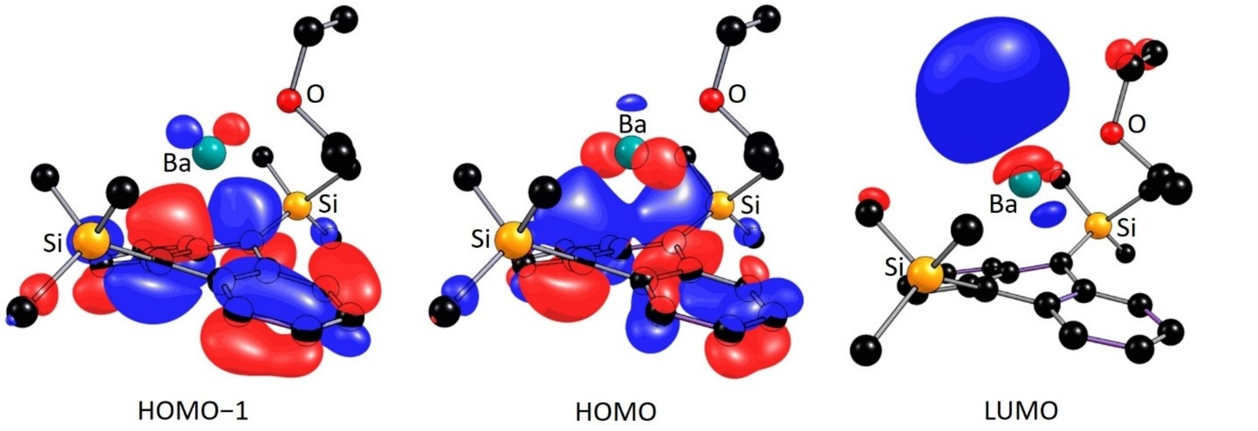

Figure 2. Visualisations of the frontier Kohn-Sham molecular orbitals for a monomeric model of **1⋅Et$_2$O** (M06-2X(D3)/Def2-TZVPP).

The ^{1}H NMR spectrum of a purple solution of **1⋅Et$_2$O** in benzene-d_6 displays two pairs of mutually coupling multiplet signals (6.43/6.11 ppm and 5.86/5.35 ppm) of two protons each, assigned to the aromatic C–H environments, and one singlet at 0.36 ppm integrating to 18 protons assigned to the Me$_3$Si-substituents. The two pairs of aromatic multiplet signals indicate an asymmetric Anth″ ligand in which, like the crystal structure, the symmetry is broken by Ba coordination to one of the outer rings, resulting in the polarisation of negative charge into this ring and an upfield shift of ^{1}H signals below 6 ppm.[43] A similar trend was observed for the aromatic signals in Mg(Anth″)⋅(THF)$_2$ (6.50 and 6.75 ppm, THF-d_8).[28] They are, however, not as far shifted as those for the anthracene dianion in Na$_2$(Anth) (3.36 and 4.25 ppm, THF-d_8).[44] Unfortunately, solvent and ligand incompatibilities preclude a more direct comparison of these species by NMR spectroscopy.

Regardless of the solvent used for crystallisation (benzene, toluene, or Et$_2$O), the ^{1}H, ^{13}C and ^{29}Si NMR shifts measured in benzene-d_6 are identical. This is explained by complete substitution of the neutral ligand (benzene, toluene, or Et$_2$O) by benzene-d_6, as supported by additional signals for the free neutral ligand, and is in agreement with the strong preference for interaction of Ba^{2+}, a soft cation, with soft arene ligands.[43b,45] ^{1}H NMR spectra of **1⋅Et$_2$O** in toluene-d_8 in the temperature range of −70 to +50 °C show hardly any changes (Figure S18). At higher temperatures, a new set of small signals indicates formation of a second species but even at +50 °C asymmetric Ba–Anth″ bonding is observed. Higher temperatures could not be applied due to limited complex stability. Already at room temperature, some decomposition (ca. 5 %) to free Anth″ is usually observed due to the extreme sensitivity of the compound.

DOSY NMR measurements on crystalline **1⋅Et$_2$O** in benzene-d_6 show that there is no interaction between the diethyl ether and **1**, presumably due to exchange with benzene-d_6 capping the Ba^{2+} ion to give **1⋅benzene**. Using Stalke's method for molecular weight determination,[46] the estimated value of 1596 g mol^{-1} is in good agreement with a trimeric structure: [Ba(Anth″)⋅(C$_6$D$_6$)]$_3$ (MW = 1632 g mol^{-1}). The deviation of 2.3 % fits with values for Et$_2$O (found: 75 g mol^{-1}, 1.3 % deviation) and remains of pentane (found: 70 g mol^{-1}, 2.8 % deviation), used to wash the crystals. From this, it is clear that the octameric solid state structure of **1⋅Et$_2$O** is not retained in benzene solution, and that the nature of the coordinated solvent and the temperature influence the nuclearity of the complex.

A monomeric model Ba(Anth″)·Et$_2$O, extracted from the crystal structure of **1⋅Et$_2$O**, was optimised by density functional theory (DFT) at the M06-2X(D3)/Def2-TZVPP level of theory, which includes dispersion corrections.[47–49] In contrast to the octameric solid-state structure, Ba bridges the 9 and 10 positions of Anth″ symmetrically, whilst Et$_2$O prefers to reside over one of the flanking rings. Natural population analysis (NPA) assigns a charge of +1.70 to Ba and −1.70 to Anth″, showing that bonding is ca. 85 % ionic. This fits well within the usual range of +1.7 to +1.8 charges for Ba^{2+} in amide or hydride complexes[50] but is considerably higher than the charge of +1.40 in the *tris*-benzene complex Ba(C$_6$H$_6$)$_3$,[7c] showing that it is considerably more facile to transfer the two Ba valence electrons to one Anth″ ligand than to three benzene ligands. The formation of Ba(Anth″) from Ba^0 atoms and Anth″ is quite exothermic: $\Delta H = -47.6$ kcal mol^{-1} ($\Delta G_{298} = -40.0$ kcal mol^{-1}). However, these are gas phase values and if one considers the atomisation enthalpy for Ba metal ($\Delta H = 43.0$ kcal mol^{-1}),[33] the thermodynamic advantages of MVS over solution methods can be clearly observed.

Although the Ba^{2+}/Anth″$^{2-}$ bond is mainly ionic, there is a small covalent contribution. The frontier Kohn–Sham molecular orbitals show that the HOMO and HOMO–1 exhibit overlap of Ba d_{xz} and $d_x2_{-y}2$ orbitals respectively with the C p-orbitals of Anth″ (Figure 2). The calculated natural electronic configuration for Ba, [Xe]6 s$^{0.06}$5d$^{0.22}$6p$^{0.01}$, indicates that barium is mainly using low-lying d-orbitals to interact with Anth″. The first unoccupied orbital (LUMO) is an sp-hybrid orbital located on Ba, protruding in the free coordination space and explaining further aggregation.

Preliminary reactivity studies show that **1·benzene** reacts by two-electron oxidation, typical for elemental Ba^0. Reactions with Ph$_2$C=NPh, H$_2$ or air all resulted in formation of Anth″. Although bulk Ba metal only reacts with H$_2$ to BaH$_2$

at high temperature,[51] **1·benzene** reacted either in benzene solution or as a solid instantaneously with only one bar H_2 at room temperature to give Anth″ and BaH_2 (the latter was proven by deuterolysis with D_2O and detection of H–D; Figure S23). ^{1}H NMR analysis revealed complete conversion to Anth″ with no evidence for dihydro-anthracene formation. In stark contrast, Mg(Anth)·$(THF)_3$ reacted only slowly with H_2 to give MgH_2 and Anth-H_2.[18,23] As described previously for the reaction of $Ph_2C{=}NPh$ with activated Ba^0,[30a] **1·benzene** was also found to enable the immediate two-electron reduction of $Ph_2C{=}NPh$ to produce Ba^{2+}, $Ph_2C{-}NPh^{2-}$ and free Anth". In presence of THF, the Ba complex crystallized as the dimer $[(Ph_2CNPh)Ba\cdot(THF)_3]_2$, which previously has been fully characterized.[30a]

This preliminary communication describes the first isolation and full characterisation of a Ba-anthracene complex (**1**), accessible by means of metal vapour synthesis. Its octameric cyclic structure is testimony to the rich structural variation of *s*-block metal complexes. Theoretical calculations are in agreement with ionic Ba^{2+}/Anth$''^{2-}$ bonding but analysis of the small covalent contributions revealed considerable Ba *d*-orbital occupation. Although the oxidation state of Ba in **1** is close to +II, its instant reactivity with H_2 under release of Anth″ nicely exemplifies the thermodynamic advantages of a hydrocarbon-soluble molecular Ba^0 synthon. Reactivity studies of **1** and syntheses of further Ba^0 synthons are currently in progress.

Electronic Supporting Information available

Experimental details, NMR spectra, crystallographic details including ORTEP,[52] details for DFT calculations. The authors have cited additional references within the Supporting Information.[53–62]

Acknowledgements

We acknowledge the Alexander von Humboldt Stiftung for supporting this project with a post-doctoral fellowship (O. P. E. Townrow). Open Access funding enabled and organized by Projekt DEAL.

Conflict of Interest

The authors declare no competing financial interest.

Data Availability Statement

The data that support the findings of this study are available in the supplementary material of this article.

Keywords: Barium · Cyclic Organometallics · Low-Valent · Metal Vapour Synthesis · Reducing Agents

[1] Alkaline-Earth Metal Compounds: Oddities and Applications, *Topics in Organometallic Chemistry 45* (Ed.: S. Harder), Springer-Verlag, Berlin, **2013**.
[2] *Early Main Group Metal Catalysis: Concepts and Reactions* (Ed.: S. Harder), Wiley-VCH, Weinheim, **2019**.
[3] a) C. Jones, *Commun. Chem.* **2020**, *3*, 159; b) B. Rösch, S. Harder, *Chem. Commun.* **2021**, *57*, 9354–9365; c) L. A. Freeman, J. E. Walley, R. J. Gilliard, *Nat. Synth.* **2022**, *1*, 439–448.
[4] a) M. Arrowsmith, H. Braunschweig, M. A. Celik, T. Dellermann, R. D. Dewhurst, W. C. Ewing, K. Hammond, T. Kramer, I. Krummenacher, J. Mies, K. Radacki, J. K. Schuster, *Nat. Chem.* **2016**, *8*, 890–894; b) G. Wang, J. E. Walley, D. A. Dickie, S. Pan, G. Frenking, R. J. Gilliard, *J. Am. Chem. Soc.* **2020**, *142*, 4560–4564; c) J. T. Boronski, A. E. Crumpton, L. L. Wales, S. Aldridge, *Science* **2023**, *380*, 1147–1149.
[5] a) S. P. Green, C. Jones, A. Stasch, *Science* **2007**, *318*, 1754–1757; b) B. Rösch, T. X. Gentner, J. Eyselein, J. Langer, H. Elsen, S. Harder, *Nature* **2021**, *592*, 717–721.
[6] S. Krieck, H. Görls, L. Yu, M. Reiher, M. Westerhausen, *J. Am. Chem. Soc.* **2009**, *131*, 2977–2985.
[7] a) X. Wu, L. Zhao, J. Jin, S. Pan, W. Li, X. Jin, G. Wang, M. Zhou, G. Frenking, *Science* **2019**, *365*, 912–916; b) Q. Wang, S. Pan, S. Lei, J. Jin, G. Deng, G. Wang, L. Zhao, M. Zhou, G. Frenking, *Nat. Commun.* **2019**, *10*, 3375; c) Q. Wang, S. Pan, Y. B. Wu, G. Deng, J. H. Bian, G. Wang, L. Zhao, M. Zhou, G. Frenking, *Angew. Chem. Int. Ed.* **2019**, *58*, 17365–17374.
[8] W. Huang, P. L. Diaconescu, *Dalton Trans.* **2015**, *44*, 15360–15371.
[9] D. Jędrzkiewicz, J. Mai, J. Langer, Z. Mathe, N. Patel, S. DeBeer, S. Harder, *Angew. Chem. Int. Ed.* **2022**, *61*, e202200511.
[10] a) M. Gimferrer, S. Danes, E. Vos, C. B. Yildiz, I. Corral, A. Jana, P. Salvador, D. M. Andrada, *Chem. Sci.* **2022**, *13*, 6583–6591; b) S. Pan, G. Frenking, *Chem. Sci.* **2023**, *14*, 379–383.
[11] B. Rösch, T. X. Gentner, J. Langer, C. Färber, J. Eyselein, L. Zhao, C. Ding, G. Frenking, S. Harder, *Science* **2021**, *371*, 1125–1128.
[12] a) C. R. Landis, R. P. Hughes, F. Weinhold, *Science* **2019**, *365*, eaay2355; b) L. Zhao, S. Pan, M. Zhou, G. Frenking, *Science* **2019**, *365*, eaay5021.
[13] a) R. Mondal, M. J. Evans, T. Rajeshkumar, L. Maron, C. Jones, *Angew. Chem. Int. Ed.* **2023**, *62*, e202308347; b) R. Mondal, K. Yuvaraj, T. Rajeshkumar, L. Maron, C. Jones, *Chem. Commun.* **2022**, *58*, 12665–12668.
[14] M.-A. Légaré, G. Bélanger-Chabot, R. D. Dewhurst, E. Welz, I. Krummenacher, B. Engels, H. Braunschweig, *Science* **2018**, *359*, 896–900.
[15] J. Mai, M. Morasch, D. Jędrzkiewicz, J. Langer, B. Rösch, S. Harder, *Angew. Chem. Int. Ed.* **2023**, *62*, e202212463.
[16] J. Mai, B. Rösch, J. Langer, S. Grams, M. Morasch, S. Harder, *Eur. J. Inorg. Chem.* **2023**, e202300421.
[17] E. Ramsden, U. S. Patent 3354190, **1967**.
[18] B. Bogdanović, *Acc. Chem. Res.* **1988**, *21*, 261–267.
[19] L. M. Engelhardt, S. Harvey, C. L. Hasten, A. H. White, *J. Organomet. Chem.* **1988**, *341*, 39–51.
[20] B. Bogdanović, N. Janke, C. Krüger, R. Mynott, K. Schlichte, U. Westeppe, *Angew. Chem. Int. Ed. Engl.* **1985**, *24*, 960–961.
[21] a) M. J. Gallagher, S. Harvey, C. L. Raston, R. E. Sue, *J. Chem. Soc. Chem. Commun.* **1988**, 289–290; b) S. Itsuno, G. D. Darling, H. D. H. Stover, J. M. J. Fréchet, *J. Org. Chem.* **1987**, *52*, 4644–4645.
[22] J. Scholz, K. H. Thiele, *J. Organomet. Chem.* **1986**, *314*, 7–11.
[23] B. Bogdanović, S. Liao, M. Schwickardi, P. Sikorsky, B. Spliethoff, *Angew. Chem. Int. Ed. Engl.* **1980**, *19*, 818–819.
[24] A. R. Utke, R. T. Sanderson, *J. Org. Chem.* **1964**, *29*, 1261–1264.

[25] C. D. Stevenson, M. P. Espe, T. Emanuelson, *J. Org. Chem.* **1985**, *50*, 4289–4291.
[26] H. Bönnemann, B. Bogdanović, R. Brinkmann, N. Egeler, R. Benn, I. Topalovic, K. Seevogel, *Main Group Met. Chem.* **1990**, *13*, 341–362.
[27] H. Lehmkuhl, A. Shakoor, K. Mehler, C. Krüger, K. Angermund, Y.-H. Tsay, *Chem. Ber.* **1985**, *118*, 4239–4247.
[28] T. Alonso, S. Harvey, P. C. Junk, C. L. Raston, B. W. Skelton, A. H. White, *Organometallics* **1987**, *6*, 2110–2116.
[29] A. F. Holleman, E. Wiberg, N. Wiberg in *Lehrbuch der Anorganischen Chemie*, 102nd ed, de Gruyter, Berlin, **2007**, pp. 2146–2147.
[30] a) P. Stegner, C. Färber, U. Zenneck, C. Knüpfer, J. Eyselein, M. Wiesinger, S. Harder, *Angew. Chem. Int. Ed.* **2021**, *60*, 4252–4258; b) P. L. Timms, *J. Chem. Educ.* **1972**, *49*, 782–784.
[31] a) M. Wiesinger, B. Maitland, C. Färber, G. Ballmann, C. Fischer, H. Elsen, S. Harder, *Angew. Chem. Int. Ed.* **2017**, *56*, 16654–16659; b) A. S. S. Wilson, M. S. Hill, M. F. Mahon, C. Dinoi, L. Maron, *Science* **2017**, *358*, 1168–1171; c) B. Rösch, T. X. Gentner, H. Elsen, C. A. Fischer, J. Langer, M. Wiesinger, S. Harder, *Angew. Chem. Int. Ed.* **2019**, *58*, 5396–5401; d) T. Höllerhage, A. Carpentier, T. P. Spaniol, L. Maron, U. Englert, J. Okuda, *Chem. Commun.* **2021**, *57*, 6316–6319; e) X. Shi, C. Hou, C. Zhou, Y. Song, J. Cheng, *Angew. Chem. Int. Ed.* **2017**, *56*, 16650–16653.
[32] M. Westerhausen, A. Koch, H. Görls, S. Krieck, *Chem. Eur. J.* **2017**, *23*, 1456–1483.
[33] The atomization enthalpy generally decreases with metal size but in group 2 shows a discrepancy for Mg and Ba (values in kJ mol^{-1} taken from ref. 29): Be 324.6, Mg 147.7, Ca 178.2, Sr 164.4, Ba 180.0.
[34] a) P. L. Timms, *Proc. R. Soc. London Ser. A* **1984**, *396*, 1–19; b) U. Zenneck, *Chem. Unserer Zeit* **1993**, *27*, 208–219.
[35] F. G. N. Cloke, P. L. Arnold, in *Comprehensive Organometallic Chemistry III* (Eds.: R. H. Crabtree, D. M. P. Mingos), Elsevier Ltd, Amsterdam, **2007**, pp. 219–238.
[36] a) D. S. Hutchings, P. C. Junk, W. C. Patalinghug, C. L. Raston, A. H. White, *J. Chem. Soc. Chem. Commun.* **1989**, 973–974; b) T. P. Hanusa, *Polyhedron* **1990**, *9*, 1345–1362.
[37] R. Mackenzie, P. L. Timms, *J. Chem. Soc. Chem. Commun.* **1974**, 650.
[38] a) K. Mochida, Y. Hiraga, H. Takeuchi, H. Ogawa, *Organometallics* **1987**, *6*, 2293–2297; b) J. P. Dunne, M. Tacke, C. Selinka, D. Stalke, *Eur. J. Inorg. Chem.* **2003**, 1416–1425.
[39] X. Sun, A. Hinz, *Inorg. Chem.* **2023**, *62*, 10249–10255.
[40] a) M. M. Olmstead, W. J. Grigsby, D. R. Chacon, T. Hascall, P. P. Power, *Inorg. Chim. Acta* **1996**, *251*, 273–284; b) J. Langer, B. Maitland, S. Grams, A. Ciucka, J. Pahl, H. Elsen, S. Harder, *Angew. Chem. Int. Ed.* **2017**, *56*, 5021–5025.
[41] L. Münzfeld, S. Gillhuber, A. Hauser, S. Lebedkin, P. Hädinger, N. D. Knöfel, C. Zovko, M. T. Gamer, F. Weigend, M. M. Kappes, P. W. Roesky, *Nature* **2023**, *620*, 92–96.
[42] H. Bock, M. Ansari, N. Nagel, R. F. C. Claridge, *J. Organomet. Chem.* **1995**, *501*, 53–60.
[43] a) S. Harder, C. Ruspic, N. Ní Bhriain, F. Berkermann, M. Schürmann, *Z. Naturforsch.* **2008**, *63*, 267–274; b) B. Rösch, J. Martin, J. Eyselein, J. Langer, M. Wiesinger, S. Harder, *Organometallics* **2021**, *40*, 1395–1401.
[44] R. G. Lawler, C. V. Ristagno, *J. Am. Chem. Soc.* **1969**, *91*, 1534–1535.
[45] a) L. Orzechowski, S. Harder, *Organometallics* **2007**, *26*, 5501–5506; b) S. Harder, M. Lutz, *Organometallics* **1997**, *16*, 225–230.
[46] a) R. Neufeld, D. Stalke, *Chem. Sci.* **2015**, *6*, 3354–3364; b) S. Bachmann, R. Neufeld, M. Dzemski, D. Stalke, *Chem. Eur. J.* **2016**, *22*, 8462–8465; c) A. K. Kreyenschmidt, S. Bachmann, T. Niklas, D. Stalke, *ChemistrySelect* **2017**, *2*, 6957–6960.
[47] Y. Zhao, D. G. Truhlar, *Theor. Chem. Acc.* **2008**, *120*, 215–241.
[48] F. Weigend, R. Ahlrichs, *Phys. Chem. Chem. Phys.* **2005**, *7*, 3297–3305.
[49] S. Grimme, J. Antony, S. Ehrlich, H. Krieg, *J. Chem. Phys.* **2010**, *132*, 154104.
[50] M. Wiesinger, C. Knüpfer, H. Elsen, J. Mai, J. Langer, S. Harder, *ChemCatChem* **2021**, *13*, 4567–4577.
[51] W. C. Schumb, E. F. Sewell, A. S. Eisenstein, *J. Am. Chem. Soc.* **1947**, *69*, 2029–2033.
[52] Deposition number 2305561 (**1·Et_2O**) contains the supplementary crystallographic data for this paper. These data are provided free of charge by the joint Cambridge Crystallographic Data Centre and Fachinformationszentrum Karlsruhe Access Structures service.
[53] R. Wang, M. Ma, X. Gong, G. B. Panetti, X. Fan, P. J. Walsh, *Org. Lett.* **2018**, *20*, 2433–2436.
[54] V. Mahendra, F. J. Davis, P. Hadley, A. Gilbert, *ISRN Mater. Sci.* **2013**, *2013*, 604132.
[55] J. Cosier, A. M. Glazer, *J. Appl. Crystallogr.* **1986**, *19*, 105–107.
[56] Rigaku Oxford Diffraction, **2023**, CrysAlisPro Software system, version 1.171.42.90a, Rigaku Corporation, Oxford, UK.
[57] O. V. Dolomanov, L. J. Bourhis, R. J. Gildea, J. A. K. Howard, H. Puschmann, *J. Appl. Crystallogr.* **2009**, *42*, 339–341.
[58] G. M. Sheldrick, *Acta Crystallogr. Sect. A* **2015**, *71*, 3–8.
[59] G. M. Sheldrick, *Acta Crystallogr. Sect. C* **2015**, *71*, 3–8.
[60] A. L. Spek, *J. Appl. Crystallogr.* **2003**, *36*, 7–13.
[61] Gaussian 16, Revision A.03, M. J. Frisch, G. W. Trucks, H. B. Schlegel, G. E. Scuseria, M. A. Robb, J. R. Cheeseman, G. Scalmani, V. Barone, G. A. Petersson, H. Nakatsuji, X. Li, M. Caricato, A. V. Marenich, J. Bloino, B. G. Janesko, R. Gomperts, B. Mennucci, H. P. Hratchian, J. V. Ortiz, A. F. Izmaylov, J. L. Sonnenberg, D. Williams-Young, F. Ding, F. Lipparini, F. Egidi, J. Goings, B. Peng, A. Petrone, T. Henderson, D. Ranasinghe, V. G. Zakrzewski, J. Gao, N. Rega, G. Zheng, W. Liang, M. Hada, M. Ehara, K. Toyota, R. Fukuda, J. Hasegawa, M. Ishida, T. Nakajima, Y. Honda, O. Kitao, H. Nakai, T. Vreven, K. Throssell, J. A. Montgomery, Jr, J. E. Peralta, F. Ogliaro, M. J. Bearpark, J. J. Heyd, E. N. Brothers, K. N. Kudin, V. N. Staroverov, T. A. Keith, R. Kobayashi, J. Normand, K. Raghavachari, A. P. Rendell, J. C. Burant, S. S. Iyengar, J. Tomasi, M. Cossi, J. M. Millam, M. Klene, C. Adamo, R. Cammi, J. W. Ochterski, R. L. Martin, K. Morokuma, O. Farkas, J. B. Foresman, D. J. Fox, Gaussian, Inc, Wallingford CT, 2016.
[62] NBO 7.0, E. D. Glendening, J, K. Badenhoop, A. E. Reed, J. E. Carpenter, J. A. Bohmann, C. M. Morales, P. Karafiloglou, C. R. Landis, F. Weinhold, Theoretical Chemistry Institute, University of Wisconsin, Madison, WI, 2018.

Manuscript received: December 1, 2023
Accepted manuscript online: December 11, 2023
Version of record online: December 22, 2023